Growth Path of Small Surface-Cracks in Ultrafine Grained Copper under Cyclic Loading

M. Goto[1], Y. Ando[1], S. Z. Han[2], T. Yakushiji[3] and N. Kawagoishi[4]

[1] *Dept. of Mech. Eng., Oita Univ., Oita, 870-1192, Japan,* masagoto@cc.oita-u.ac.jp
[2] *Korea Institute of Mater. Sci., Changwon, Kyungnam, 641-831, Korea,* szhan@kmail.kims.re.kr
[3] *Dept. of Mech. Eng., Oita National College of Tech., Oita, 870-0152 Japan,* yakusiji@oita-ct.ac.jp
[4] *Dept. of Mech. Eng., Kagoshima Univ., Kagoshima, 890-0065, Japan,* hiro@mech.kagoshima-u.ac.jp

ABSTRACT. *High-cycle fatigue tests were carried out on specimens of ultrafine grained copper produced by equal channel angular pressing. The formation behavior of surface damage and the growth behavior of a small surface-crack were monitored. A major crack, which led to the final fracture of the specimen, initiated from shear bands (SBs). Propagation behavior of the major crack was influenced by damage ahead of the crack tip, and consequently different morphologies of the crack growth paths developed, depending on the stress amplitude. The physical background of growth path formation was discussed from the viewpoint of the evolution of surface damage.*

INTRODUCTION

It has been shown that ultrafine grained (UFG) metals produced by severe plastic deformation (SPD) techniques, such as ECAP (equal channel angular pressing) [1-4], can have unique and novel fatigue characteristics. There has been interest in such characteristics as the cyclic stress-strain response, softening property, and formation of shear bands (SBs). Since the fatigue life of components of machines and structures are mainly controlled by the growth life of a fatigue crack, the crack growth behavior should be clarified for the design of safe members in machines and structures. Recently, the growth behaviors of millimeter-range cracks in UFG metals were studied for compact-tension [5,6] and single edge notched specimens [7,8]. On the other hand, the fatigue life of smooth specimens is approximately controlled by the growth life of a small surface-crack. Nisitani and Goto [9,10] showed the crack growth life from an initial size to 1 mm accounted for about 70% of the fatigue life of plain specimens of many conventional grain-sized (CGS) metals. This means the growth behavior of small cracks must be clarified to estimate the fatigue life of plain members. However, little has been reported on the growth behavior of small surface-cracks in UFG metals.

For CGS metals, meanwhile, it has been reported that the propagation of a small surface-crack is frequently arrested owing to microstructural inhomogeneities such as grain boundaries (GBs), phase boundaries, precipitations, and inclusions [11-13]. Furthermore, the arresting (retardation/stopping) was remarkably large for a crack smaller than ten times the grain size [14], whereas it was negligibly small for a larger crack. In the present study on UFG metals, ten times the grain size is roughly equivalent to a few micrometers and is much less than the grain sizes of CGS counterparts (a few tens of micrometers). Following the example of arresting crack growth in CGS metals, it thus appears the microstructural inhomogeneity of UFG metals has a negligible effect on the growth behavior of cracks larger than the grain sizes of CGS counterparts. With respect to the microstructure in UFG copper, Segal [1] has shown an oriented distribution of defects along the shear plane of pressing. Here, the defects refer to dislocations, GBs and cellular substructures. Correspondingly, it has been reported the primary SBs of post-fatigued UFG copper formed along the shear direction of the final ECAP [15-17]. Therefore, such microstructural inhomogeneity resulting from ECAP should affect the behavior of a fatigue crack, even a crack larger than a conventional grain. Zhang et al. [18] carried out low-cycle fatigue tests for UFG Al-0.7wt% Cu under constant plastic strain control, showing the growth paths of fatigue cracks nucleated either along SBs or along the coarse deformation bands, depending on the applied strain amplitude. In addition, it has been shown that cracks in UFG copper under low-cycle fatigue propagate along SBs [19,20]. For the high-cycle fatigue regime, to the authors' knowledge, there has been little reported in the literature on the effect of microstructural inhomogeneity on the behavior of fatigue surface-cracks in UFG metals.

In the present study, stress-controlled fatigue tests for UFG copper were conducted. The formation behavior of SBs and growth behavior of a small crack were monitored to clarify the effect of microstructural inhomogeneity on the growth path of a major crack leading to the final fracture of the specimen.

EXPERIMENTAL PROCEDURES

The material used was pure oxygen-free copper (OFC, 99.99 wt% Cu). Prior to ECAP, the materials were annealed at 500˚C for 1 hr (grain size: 100 μm). The inner and outer angles of the channel intersection in the ECAP die were 90 and 45˚, respectively. Repetitive ECAP was accomplished according to the Bc route (after each pressing, the billet bar was rotated around its longitudinal axis through 90˚). Twelve passages of extrusion resulted in an equivalent shear strain of about 11.7 [21]. MoS_2 was used as lubricant for each pressing, and the pressing speed was 5 mm/sec. The mechanical properties before ECAP were 232 MPa tensile strength, 65% elongation, and a Vickers hardness number of 63. After twelve passages of ECAP, the properties changed to 443 MPa, 32 %, and 131, respectively. Transverse cross sections of the processed bars were cut to prepare the specimens for transmission electron microscopic observation. Specimens were mechanically polished to a thickness of 100 μm and then subjected to

twin-jet electropolishing using a solution comprising 200 ml CH_3OH and 100 ml HNO_3. The jet thinning was conducted at –30˚C.

Round bar specimens 5 mm in diameter were machined from the processed bars. Before testing, all fatigue specimens were electrolytically polished (~ 25 μm from the surface layer) prior to mechanical testing in order to remove any preparation affected surface layer. Polishing was carried out at 25 ˚C using an electrolyte consisting of 600 ml phosphoric acid, 300 ml distilled water and 100 ml sulfuric acid. All tests were carried out at room temperature using a rotating bending fatigue machine operating at 50 Hz. Observations of fatigue damage on the specimen surface were performed using optical microscopy (OM). The crack length, l, is a length measured along the circumferential direction of the surface (refer to the inset of Fig. 4). The measurement of crack length was conducted using a plastic replication technique.

RESULTS AND DISCUSSION

Figure 1 shows typical microstructure of the test material obtained using transmission electron microscopy (TEM), complete with selected area diffraction patterns (SADPs) of the central area of the materials (1 μm in diameter). In the UFG copper, granular grains with an average size of 300 nm were observed. The GBs of some grains had lost their sharpness and exhibited a 'spotty' contrast and broad contours, suggesting that GBs contain random networks of GB dislocations [22]. The SADPs consisted of rings of diffraction spots, showing that GBs have high angles of misorientation.

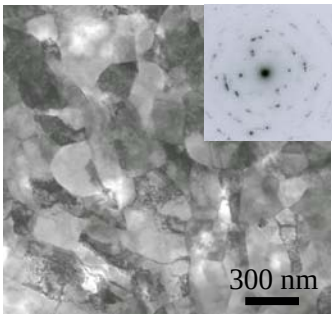

Figure 1. TEM micrograph of ECAP-processed copper.

Fatigue tests were carried out at σ_a = 100, 120, 200 and 240 MPa, where the number of cycles to failure, N_f, at corresponding stress amplitudes were $N_f = 3.04 \times 10^6$, 1.63×10^6, 3.14×10^5 and 1.68×10^5 cycles, respectively. Fig. 2 shows the growth curve ($\ln l$ vs. N) of a major crack. Under low stress (Fig. 2a), the crack length increased sharply in the initial stage of stressing, and this was followed by a change in the slope of the growth curve around l = 0.1-0.3 mm. Specifically, the actual crack length after the slope change was smaller than the length expected from an extension of the growth curve in the range l < 0.1 mm, showing a decreased crack growth rate (CGR). However, such retarded

growth ceased before the crack length reached about l = 0.4 mm, and the CGR was restored and growth curves could be approximated as straight lines (l > 0.4 mm). Under high stress (Fig. 2b), there was no significant retardation of crack growth. The initial growth curve could be approximated as a slightly concave line, followed by a straight line for a large crack length (l > 0.3 mm). That is, the CGR accelerated with an increase in the crack length.

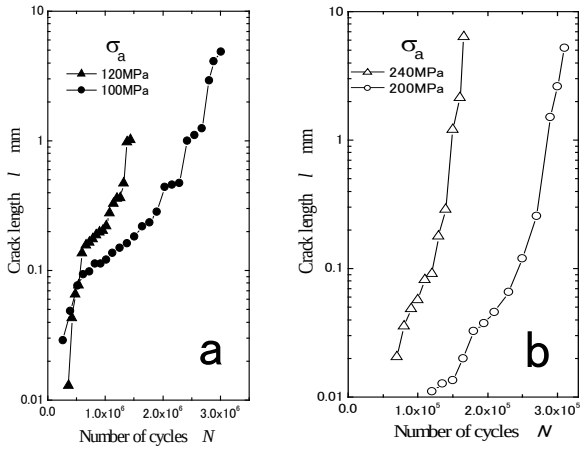

Figure 2. Crack growth data: (a) σ_a = 100 and 120 MPa, (b) σ_a = 200 and 240 MPa.

To clarify the formation of surface damage, the change in surface states during stressing was monitored by OM. Fig. 3 shows the formation process of surface damage at σ_a = 120 MPa. It showed that primary SBs form at an early stage of cycling; in particular, the morphology of SBs at a high stress amplitude (σ_a > 200 MPa) can be classified into persistent slip band (PSB)-like SBs [15,17]. The number and area of the damaged regions slowly increase with further cycling up to a specific cycle ratio, depending on the stress amplitude; e.g. $N/N_f \approx 0.4$ and 0.2 for σ_a = 120 and 240 MPa, respectively. Once this specific cycle ratio is exceeded, both the number and area of the damaged regions significantly rise. The damaged region formed after the specific cycle ratio is reached is roughly classified as a secondary SB [20] and insular damage with a complex morphological feature [17]. In addition, the change in surface Vickers hardness (load: 2.9 N) during repeated stressing was studied. The surface hardness showed an initial moderate reduction and subsequently a significant reduction. By investigating the change in surface hardness and the formation of surface damage together, it was found this considerably large drop in hardness is closely related to the significant formation of damaged areas. Several studies on the GBs of UFG copper prepared by SPD have suggested the existence of highly non-equilibrium GBs with high energy, excess volume, and long-range stress fields, etc. [22,23], where the absorption of dislocations into GBs takes place with remarkably enhanced diffusion [23]. The initial (gentle) hardness drop appears to result mainly from a release of strain energy relating to primary SB formation and a decrease in the density of dislocations inside the grains. A

very large decrease in hardness has been attributed to a release of strain energy resulting from heavy surface damage due to GB sliding [24]. Incidentally, the time taken for a significant increase in surface damage at σ_a = 100 MPa nearly corresponded to the duration of the retardation in crack growth.

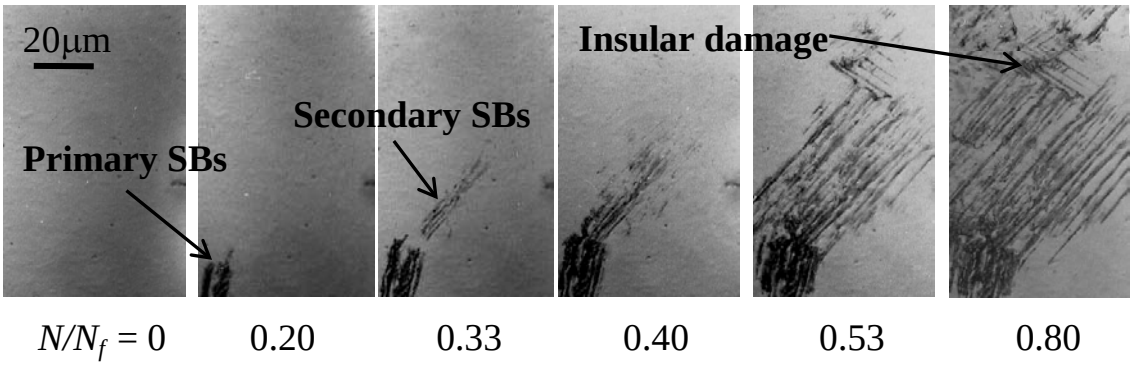

Figure 3. Formation process of surface damage at σ_a = 120 MPa.

To study the reason for transient retarded growth for a major crack at a low stress amplitude, the change in the morphological features in a region around and ahead of the crack tip were monitored (Fig. 4). Specifically, supplemental fatigue tests for the monitoring were conducted at σ_a = 100 and 240 MPa. Figs.4 (a) and (b) show the change in the surface states at σ_a = 100 and 240 MPa, respectively. At σ_a = 100 MPa, after a micrometer-range crack initiated from primary SBs, the crack propagated along

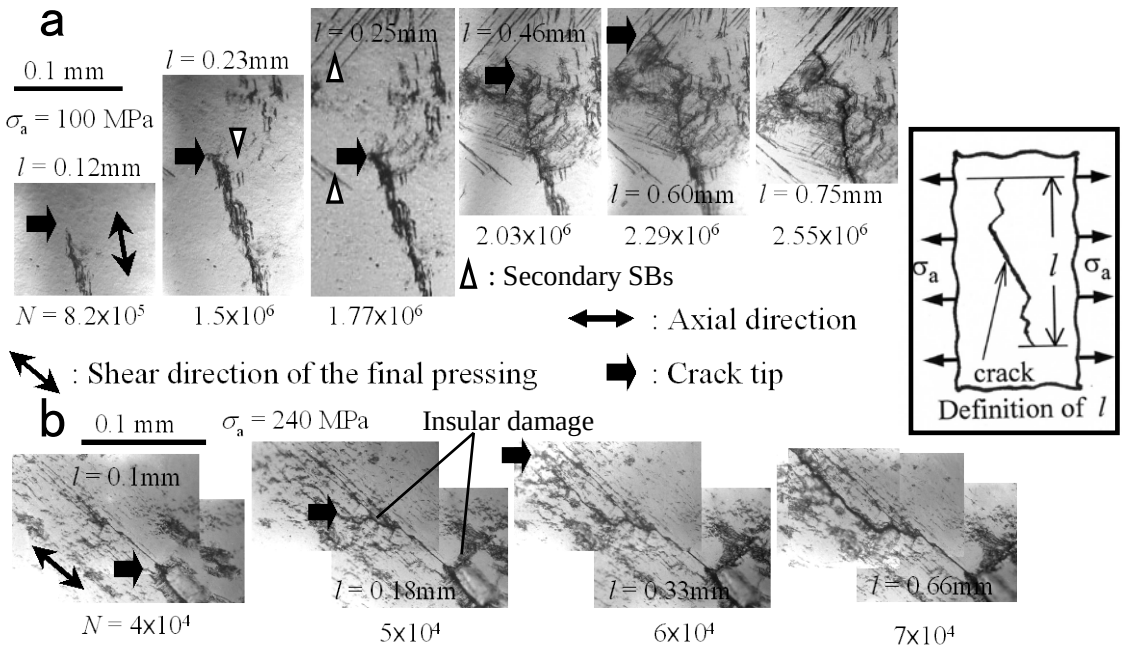

Figure 4. Change in fatigue damage around and ahead of a major crack tip during stressing, and the crack growth path on a micro-scale: (a) σ_a = 100 MPa, (b) σ_a = 240 MPa.

the primary SBs and its length reached l = 0.23 mm at N = 1.5x10^6. The crack growth then retarded with the formation of secondary SBs ahead of the crack tip. Blocking of crack growth and a change in the growth direction occurred when the crack tip reached the secondary SBs, resulting in a torturous zigzag crack growth path with branchings. Such a growth path may be convenient for roughness-induced crack closure, which contributes to a decrease in CGR, but the retarded growth behavior was transient. Since the driving force of crack growth is enhanced with an increase in crack length, the influence of secondary SBs on the growth behavior appears to be negligible for a crack larger than l = 0.4 mm (Fig. 2). On the other hand, a major crack at σ_a = 240 MPa has been initiated from PSB-like SBs, which formed at an early stage of cycling along the shear direction of the final pressing [25]. After initiation, the crack propagated along the orientation of PSB-like SBs, and the crack length reached l = 0.1 mm at N = 4x10^4 (Fig. 4b). At this stage, a number of microcracks formed from PSB-like SBs were distributed ahead of a major crack tip. The subsequent stressing resulted in the formation of insular damage with different orientations to the PSB-like SB orientations, whereas the growth behavior of a major crack was hardly affected by the insular damage. In contrast, the microcracking affected the growth behavior of the major crack. The major crack continued to propagate with coalescence of the microcracking, forming a growth path along the shear direction of the final pressing.

Figures 5 (a) and (b) show a growth path of a major crack in the specimens fatigued at σ_a = 100 (l = 4.95 mm) and 240 MPa (l = 5.55 mm), respectively. The crack formed at σ_a = 100 MPa exhibited a microscopically tortuous growth path; however, on a macro-scale, the growth path was nearly perpendicular to the axial direction of the specimen. At σ_a = 240 MPa, on a macro-scale, the crack growth path was inclined to the axial direction. This inclined path should result from the crack propagation along the shear direction of the final pressing, as illustrated in Fig. 4 (b). Thus, it can be concluded that the growth behavior of surface-cracks at a low stress amplitude is influenced initially by primary SBs and subsequently by secondary SBs, but the growth

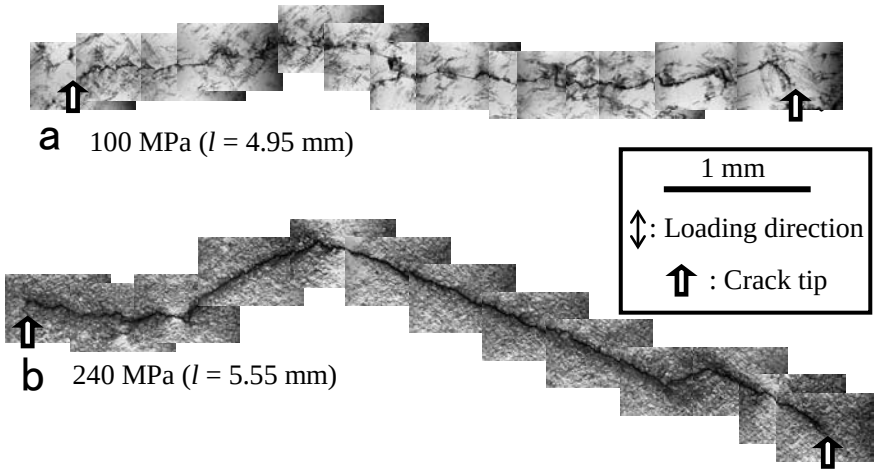

Figure 5. Macroscopic views of the crack growth path.

behavior of surface-cracks at a high stress amplitude should be mostly controlled by cracking from PSB-like SBs.

CONCLUSIONS

The main results of the present study are summarized as follows.

The crack growth behavior was closely related to the formation of SBs. At a low stress amplitude, a crack initiating from primary SBs initially propagated along the SBs. With further stressing, on a micro-scale, the crack propagated with a zigzag growth path owing to the interference of secondary SBs formed under subsequent stressing. On a macro-scale, however, the crack growth path was nearly perpendicular to the specimen axis. At a high stress amplitude, a crack initiated from PSB-like SBs formed along the shear direction of the final pressing. After initiation, the crack continued to grow along the PSB-like SBs with coalescence of microcracking from other PSB-like SBs. Although insular damage occurred after the formation of PSB-like SBs, this did not affect the macroscopic growth path. Therefore, on a macro-scale, a major crack had a torturous growth path along the shear direction of the final pressing.

ACKNOWLEDGEMENTS

This study was supported by a Grant-in-Aid (20560080) for Scientific Research from the Ministry of Education, Science, and Culture of Japan, and a grant from the Fundamental R&D Program for Core Technology of Materials funded by the Ministry of Commerce, Industry and Energy, Republic of Korea.

REFERENCES

1. Segal, V,M. (1995) *Mater. Sci. Eng.* **A197**, 157-164.
2. Valiev, R.Z. (1997) *Mater. Sci. Eng.* **A234-236**, 59-66.
3. Zhu, Y.T., Lowe, T.C. (2000) *Mater. Sci. Eng.* **A291**, 46-53.
4. Iwahashi, Y., Horita, Z., Nemoto, M. and Langdon, T.G. (1998) *Acta Mater.* **46**, 3317-3331.
5. Vinogradov, A., Nagasaki, S., Patlan, V., Kitagawa, K. and Kawazoe, M. (1999) *NanoStruct. Mater.* **11**, 925-934.
6. Pao, P.S., Jones, H.N., Cheng, S.F. and Feng, C.R. (2005) *Int. J. Fatigue*. **27**, 1164-1169.
7. Chung, C.S., Kim, J.S.,Kim, H.K. and Kim, W.J. (2002) *Mater. Sci. Eng.* **A337**, 39-44.
8. Kim, H.K., Choi, M.I., Chung, C.S. and Shin, D.H. Mater. (2003) *Sci. Eng.* **A340**, 243-250.
9. Nisitani, H., Goto, M. and Kawagoishi, N. (1992) *Eng. Fract. Mech.* **41**, 499-513.

10. Goto, M., Nisitani, H. (1994) *Fatigue Fract. Eng. Mater. Struct.* **17**, 171-185.
11. Lankford, J. (1982) *Fatigue Fract. Eng. Mater. Struct.* **5**, 233-248.
12. Tanaka, K., Hojo, M. and Nakai,Y. (1983) *ASTM-STP* **811**, 207-232.
13. Goto, M., Knowles, D.M. (1998) *Eng. Fract. Mech.* **60**, 1-18.
14. Goto, M. (1994) *Fatigue Fract. Eng. Mater. Struct.* **17**, 635-649.
15. Wu, S.D., Wang, Z.G., Jiang, C.B., Li, G.Y., Alexandrov, I.V. and Valiev, R.Z. (2003) *Scripta Mater.* **48**, 1605-1609.
16. Kunz, L., Lukáš, P. and Svoboda, M. (2006) *Mater. Sci. Eng.* **A424**, 97-104.
17. Goto, M., Han, S.Z., Yakushiji, T., Lim, C.V. and Kim, S.S. (2006) *Scripta Mater.* **54**, 2101-2106.
18. Zhang, Z.F., Wu, S.D., Li, Y.J., Liu, S.M. and Wang, Z.G. (2005) *Mater. Sci. Eng.* **A412**, 279-286.
19. Hashimoto, S., Kaneko, Y., Kitagawa, K., Vinogradov, A. and Valiev, R.Z. (1999) *Mater. Sci.Forum.* **312-314**, 593-598.
20. Maier, H.J., Gabor, P. and Karaman, I. (2005) *Mater. Sci. Eng.* **A410-411**, 457-461.
21. Iwahashi, Y., Wang, J., Horita, Z., Nemoto, M. and Langdon, T.G. (1995) *Scripta Mater.* **35**, 143-146.
22. Valiev, R.Z. (1995) *NanoStructured Mater.* **6**, 73-82.
23. Valiev, R.Z., Kozlov, E.V., Ivanov, Yu.F., Lian, J., Nazarov, A.A. and Baudelet, B. (1994) *Acta Metall. Mater.* **42**, 2467-75.
24. Goto, M., Han, S.Z., Kim, S.S. and Kawagoishi,N. C.Y. Lim. (2007) *Scripta Mater.* **57**, 293-296.
25. Goto, M., Han, S.Z., Yakushiji, T., Kim, S.S. and Lim, C.Y. (2008) *Int. J. Fatigue*. **33**, 1333-1344.